

Magnetic properties of the rare earth compounds TmPO_4 and HoVO_4 in high magnetic fields

V. A. Ioffe, S. N. Andronenko, A. N. Bazhan, S. V. Kravchenko, C. Bazan,¹⁾ B. G. Vekhter, and M. D. Kaplan

Institute of Physics Problems, Academy of Sciences of the USSR, Moscow; I. V. Grebenshchikov Institute of Silicate Chemistry, Academy of Sciences of the USSR, Leningrad; and Institute of Chemistry, Academy of Sciences of the Moldavian SSR, Kishinev

(Submitted 21 July 1982)

Zh. Eksp. Teor. Fiz. **84**, 707–718 (February 1983)

The static magnetic properties of the tetragonal rare earth compounds TmPO_4 and HoVO_4 have been investigated in magnetic fields up to 65 kOe and at temperatures from 2 to 50 K, and also in magnetic fields up to 180 kOe at 4.2 K. At low temperatures $T < 10$ K and magnetic fields $H < 10$ kOe oriented perpendicular to the [001] axis the compounds exhibit the properties of a Van Vleck paramagnet. The $\chi(H)$ dependence is linear and independent of the temperature. On increasing the magnetic field to $H > 10$ kOe, the $\chi(H)$ dependence becomes nonlinear in field and depends on the direction of H in the [001] plane; the dependences are different for TmPO_4 and HoVO_4 . The magnetic moments $\chi(H)$ for TmPO_4 in high magnetic fields are different when the field is oriented along the [100] binary axis or along the [110] binary axis. This difference may be due to effective interaction between the Tm^{3+} ions caused by Jahn-Teller interaction between these ions and the lattice distortions of the B_{2g} symmetry crystal. The observed difference between the $\chi(H)$ dependences for $\mathbf{H} \parallel [100]$ and $\mathbf{H} \parallel [110]$ and their nonlinearity for HoVO_4 can be explained by the occurrence of a nonlinear dependence of the Van Vleck magnetic moment in high magnetic fields.

PACS numbers: 75.20.Ck

INTRODUCTION

The compounds TmPO_4 and HoVO_4 belong to a large and interesting group of RXO_4 rare earth compounds with D_{4h} ¹⁹ tetragonal symmetry which have been intensely studied (where $\text{R} = \text{Tb}^{3+}$, Tm^{3+} , Ho^{3+} , ..., and $\text{X} = \text{P}$, As , V).¹⁻⁴ A Jahn-Teller transition is observed in many of these compounds on lowering the temperature, accompanied by a reduction in crystal symmetry from tetragonal to orthorhombic. The position of the energy levels of the rare earth ions in many of these compounds has been determined, both in the high-temperature and low-temperature phases, by electron paramagnetic resonance (EPR) studies and by investigation of their optical properties.¹⁻⁵

The exchange of virtual phonons between electrons of different centers of Jahn-Teller crystals and the electron-deformation interaction lead to an effective inter-site interaction, producing structural phase transitions in these systems. In cases when the electronic ground state of the Jahn-Teller ion is degenerate and the vibronic coupling constant¹ is different from zero, the structural phase transition necessarily occurs when a sufficiently low temperature has been reached. The crystal TmVO_4 is an example of such a system.² If the electronic ground state is not degenerate, interaction between sites can either arise as a result of vibronic mixing² of the ground state with an excited state which is also orbitally non-degenerate as, for example, in DyVO_4 ,⁴ or from the Jahn-Teller effect on a low lying excited level (the case of TbVO_4 ,^{1,2} where the Jahn-Teller interaction occurs for an excited doublet and there is also mixing of the ground-state singlet with the excited state). In the latter two situations, structural phase transitions only arise for sufficiently strong inter-site interaction. The Jahn-Teller phase transi-

tion in DyVO_4 , for example, occurs for $A > \epsilon$, where A is the Jahn-Teller molecular field parameter responsible for the phase transition, and ϵ is the magnitude of the level splitting in the disordered phase and occurs in TbVO_4 at $A > 1.2\epsilon$. If these conditions are not satisfied structural phase transitions do not occur, but the correlations of local Jahn-Teller distortions do, however, appreciably influence the crystal properties.

The crystal TmPO_4 , in which a strong dip (not to zero) in the temperature dependence of the elastic modulus C_{66} is found at $T = 20$ K on the basis of ultrasonic measurements,⁴ must also be included among such crystals. As was shown,⁴ this softening is due to the correlation of Jahn-Teller local deformations, produced by electron-phonon coupling and homogeneous deformation of the crystal of B_{2g} symmetry. The magnitude of this vibronic coupling is insufficient to produce a ferro-distortive phase transition but nevertheless the intercenter interaction constant, as found earlier⁴ and as will be shown later, is rather large. The correlations are consequently important not only for the acoustic but also for all other properties of TmPO_4 . We should note that the arrangement of energy levels of the Tm^{3+} and Ho^{3+} ions in these compounds is similar to the arrangement for Tb^{3+} in the TbVO_4 compound, which has been well studied by the optical method,² and for which a cooperative Jahn-Teller transition is observed at $T < T_D = (34 \pm 1)$ K. Mehran *et al.*⁵ attribute the dependence of EPR line width on temperature, observed in studying the EPR spectra of CD^{3+} ions in TmPO_4 , to B_{2g} dynamic Jahn-Teller distortions that produce a local orthorhombic environment for the rare earth ion. There has recently been great interest in studying these compounds under the action of external fields, magnetic or pressure.^{1,6,7} It is interesting to study the static magnetic

properties of TmPO_4 in a magnetic field oriented along different crystal directions coinciding with the possible [100] or [110] distortion axes. We found earlier⁷ an anomalous dependence, in fields greater than 30 kOe, of the anisotropy of the magnetic properties of TmPO_4 on the applied magnetic field on orienting \mathbf{H} along the [100] and [110] axes. The magnetic properties of HoVO_4 have been studied by NMR.⁸ The aim of the present work was to study the magnetic field dependences of the magnetic moment of TmPO_4 and HoVO_4 single-crystals for different orientations of \mathbf{H} relative to the crystallographic axes, at various temperatures, and to compare the magnetic properties of TmPO_4 and HoVO_4 .

The TmPO_4 and HoVO_4 single-crystals were grown in the Silicate Institute of the Academy of Sciences of the USSR,²⁾ contained Cd^{3+} and Eu^{3+} impurity in the starting materials, and their EPR spectra were studied. The single-crystals were oriented by an x-ray device in the Institute of Physics Problems of the Academy of Science of the USSR. The accuracy in determining the crystal axes was not worse than ³⁾ 2 to 3°.

The experiments were carried out on a vibrating-specimen magnetometer⁹ built on the Institute for Physics Problems, in the magnetic field range from 0 to 60 kOe at temperatures $1.7 < T < 60$ K, and on a magnetometer built at the International Laboratory for High Magnetic Fields and Low Temperatures (Wroclaw, Poland), in the field range from 0 to 180 kOe at $T = 4.2$ K.

EXPERIMENTAL RESULTS

We showed in Fig. 1 of the earlier publications⁷ the field dependences of the magnetic moment for TmPO_4 with \mathbf{H} oriented along the [100] binary axis—curve 1, the [110] binary axis—curve 2, and the [001] tetragonal axis—curve 3, measured at $T = 4.2$ K in magnetic fields up to 120 kOe. Subsequently the $\mathcal{M}(H)$ dependences for $\mathbf{H}||[100]$ and $\mathbf{H}||[110]$ were obtained at $T = 4.2$ K in magnetic fields varying up to 180 kOe at the International Laboratory in Wroclaw. It could be seen that the $\mathcal{M}(H)$ dependences coincide for the $\mathbf{H}||[100]$ and $\mathbf{H}||[110]$ orientations in fields up to 15 kOe and can be described by the expression $\mathcal{M}(H) = \chi H$, where $\chi = (0.4 \pm 0.02)$ cgs·mol⁻¹. An appreciable difference arises between $\mathcal{M}(H)$ for these two field directions for fields $H > 15$ kOe and these dependences become nonlinear. On increasing the magnetic field to 180 kOe the nonlinear $\mathcal{M}(H)$ dependences for both orientations tend to saturate respectively like $\mathcal{M}(H) = M_0$ with $M_0 = (3.4 \pm 0.3) \times 10^4$

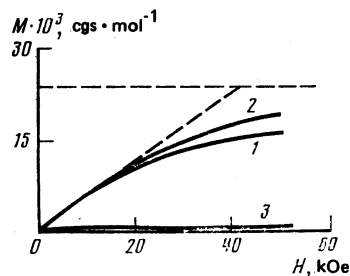


FIG. 1. Magnetic field dependence of magnetic moment for HoVO_4 for various orientations of \mathbf{H} .

cgs·mol⁻¹ and $\mathcal{M}(H) = M_0^*$ with $M_0^* = (2.4 \pm 0.3) \times 10^4$ cgs·mol⁻¹. A linear dependence $\mathcal{M}(H) = \chi^* H$ is observed for the $\mathbf{H}||[001]$ orientation, where $\chi^* = (1.5 \pm 0.2) \times 10^{-2}$ cgs·mol⁻¹. The dependences of the magnetic moment on the applied field are shown in Fig. 1 for HoVO_4 for \mathbf{H} oriented along the [100] binary axis—curve 1, along the [110] binary axis—curve 2 and along the [001] tetragonal axis—curve 3 at $T = 4.2$ K and in magnetic fields up to 65 kOe. It can be seen that in weak fields, $H < 15$ kOe, the $\mathcal{M}(H)$ dependences for $\mathbf{H}||[100]$ and $\mathbf{H}||[110]$ are the same as in TmPO_4 , represented by the expression $\mathcal{M}(H) = \chi H$ where $\chi = (0.42 \pm 0.2)$ cgs·mol⁻¹. A difference appears for fields $H > 15$ kOe between the $\mathcal{M}(H)$ dependences for $\mathbf{H}||[110]$ and $\mathbf{H}||[100]$ and the variations become non-linear. It can also be seen from Fig. 1 that the difference between the $\mathcal{M}(H)$ dependences in high fields for these two orientation is not as appreciable as for TmPO_4 . The non-linear $\mathcal{M}(H)$ dependences for $H > 15$ kOe for $\mathbf{H}||[110]$ differ appreciably for TmPO_4 and HoVO_4 . An inflection occurs in the $\mathcal{M}(H)$ dependence for TmPO_4 , i.e., the magnetic moment increases faster than linearly with field in fields $15 < H < 30$ kOe, while for $H > 30$ kOe the usual saturation is realized. No inflection is observed in the $\mathcal{M}(H)$ dependence for HoVO_4 and saturation occurs over the whole field range.

On increasing the magnetic field to $H > 40$ kOe, the non-linear $\mathcal{M}(H)$ dependences for HoVO_4 for $\mathbf{H}||[110]$ and $\mathbf{H}||[100]$ tend to saturation with $\mathcal{M}(H) = M_0$, where

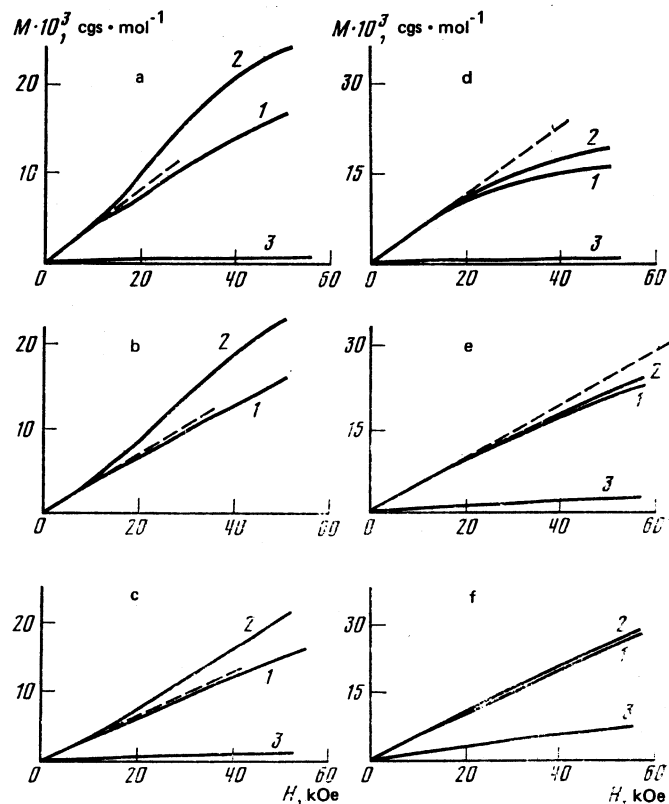


FIG. 2. Magnetic field dependence of magnetic moment for TmPO_4 (a,b,c) and HoVO_4 (d,e,f) for various orientations of \mathbf{H} (1— $\mathbf{H}||[100]$, 2— $\mathbf{H}||[110]$, 3— $\mathbf{H}||[001]$) and for various temperatures: a,d) $T = 4.2$ K; b,e) $T = 12$ K; c,f) $T = 19$ K.

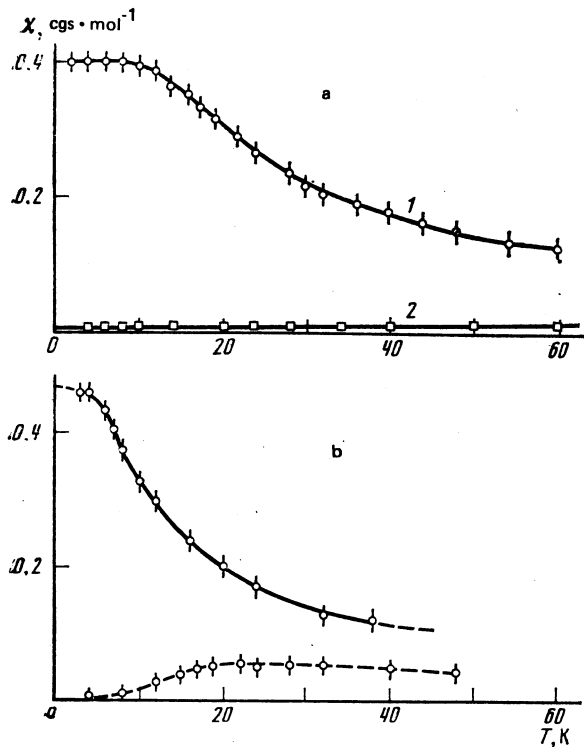


FIG. 3. Variations in magnetic susceptibility measured in weak magnetic fields for various orientation of \mathbf{H} for TmPO $_4$ (a) and HoVO $_4$ (b).

$M_0 = (2.3 \pm 0.4) 10^4$ cgs \cdot mol $^{-1}$ and $\mathcal{M}(H) = M_0^*$, where $M_0^* = (2.1 \pm 0.4) 10^4$ cgs \cdot mol $^{-1}$ respectively.

The dependences of magnetic moment \mathcal{M} on applied field \mathbf{H} are shown in Fig. 2 for TmPO $_4$ and HoVO $_4$ for various orientations of \mathbf{H} relative to the crystal axes and for various temperatures. It can be seen from Fig. 2 (curves 2) that the inflection in the nonlinear $\mathcal{M}(H)$ dependences for TmPO $_4$ for the $\mathbf{H}||[110]$ orientation becomes less marked with increasing temperature. The difference between the $\mathcal{M}(H)$ dependences for $\mathbf{H}||[110]$ and $\mathbf{H}||[100]$ then become less. It can also be seen from Fig. 2 (curves 3) that for \mathbf{H} oriented along the $[001]$ axis, an increase in magnetic moment \mathcal{M} is observed starting at temperatures $T \approx 14$ K, in contrast to TmPO $_4$ where \mathcal{M} is practically independent of temperature for this orientation of \mathbf{H} .

The temperature dependences of the magnetic susceptibility χ in weak fields $H < 15$ kOe are shown in Fig. 3, a, b, for the orientations $\mathbf{H}||[100]$ —curve 1 and $\mathbf{H}||[001]$ —curve 2 for TmPO $_4$ and HoVO $_4$ respectively, obtained by analyzing the dependences of Fig. 2 for different temperatures. It can be seen that the nature of the temperature dependence of the susceptibility of TmPO $_4$ changes at temperatures in the region of 18 K and of HoVO $_4$ at temperatures in the region of 14 K. For both HoVO $_4$ and TmPO $_4$ at low temperatures $T < 6$ K, the susceptibility χ for $\mathbf{H}||[100]$ is independent of temperatures in weak fields, which is characteristic of a Van Vleck paramagnet. On raising the temperature, a temperature dependence of susceptibility arises which for sufficiently high temperatures, $T > 30$ K, can be described by the law $\chi(T) \sim 1/T$. As has already been pointed out, the susceptibility χ^* of TmPO $_4$ for $\mathbf{H}||[001]$ is weakly temperature

dependent. For HoVO $_4$ at temperatures of the order of ~ 14 K, an increase in χ^* occurs. On increasing the temperature further to $T > 40$ K, a reduction in χ^* is observed for HoVO $_4$.

DISCUSSION OF THE RESULTS

The experimental studies have revealed anomalous field dependences of the magnetic moment of TmPO $_4$ for $\mathbf{H}||[110]$. It is natural to seek an explanation for them as the effect of correlation of Jahn-Teller local distortions, the existence of which was demonstrated in studies of the acoustic properties of this crystal.⁴ A theoretical interpretation of the features of the properties of a virtual TmPO $_4$ elastomer can be carried out within the framework of the microscopic theory of a cooperative Jahn-Teller effect.

The elementary cell in the tetragonal zircon-structure TmPO $_4$ crystal contains two equivalent Jahn-Teller ions. The group of lowest electronic states of the Tm $^{3+}$ ion, characterized by D_{2d} local symmetry, is well separated from higher lying excited states and consists of the ground and excited singlet states, between which, approximately in the middle (we neglect the small shift from the central position), lies a doublet state. The Hamiltonian of the crystal placed in an external magnetic field perpendicular to the tetragonal axis can be written in the form^{1,10,11}

$$\begin{aligned} \hat{H} = & \frac{1}{2} c_0 \Omega u^2 + \sum_k \hbar \omega_k (b_k^+ b_k + \frac{1}{2}) - g_0 (c_0 \Omega / N)^{1/2} u \sum_m \sigma_z^m \\ & - \sum_{m \neq k} i (V_{mk} b_k + V_{mk}^* b_{-k}^+) \sigma_z^m \\ & - \frac{1}{2} e \sum_m (1 + \tau_z^m) \sigma_x^m - g \beta \sum_m (H_x S_x^m + H_y S_y^m). \end{aligned} \quad (1)$$

When writing the Hamiltonian (Eq. (1)) it is considered that both sublattices of the crystal also remain equivalent on switching on the field, so that \hat{H} can be regarded as the result of summing over the sublattices. The first two terms of the Hamiltonian represent the elastic energy of the crystal deformed in the magnetic field and the normal modes. The next two terms describe electron-deformation and electron-phonon interactions with modes of B_{2g} symmetry. The term proportional to ε corresponds to the splitting of the energy levels of the Tm $^{3+}$ ions in the absence of a magnetic field. Finally, the last term represents the Zeeman interaction with the coordinate system rotated 45° around the $[001]$ axis relative to the crystallographic axes, i.e., $X || [110]$. The electron operator matrices in Eq. (1) can be written for the chosen basis of four electronic states in the form¹

$$\begin{aligned} \sigma_z = & \begin{pmatrix} 1 & 0 & 0 & 0 \\ 0 & 1 & 0 & 0 \\ 0 & 0 & -1 & 0 \\ 0 & 0 & 0 & -1 \end{pmatrix}, \quad \frac{1}{2} (1 + \tau_z) \sigma_x = \begin{pmatrix} 0 & 0 & 1 & 0 \\ 0 & 0 & 0 & 0 \\ 1 & 0 & 0 & 0 \\ 0 & 0 & 0 & 0 \end{pmatrix}, \\ S_x = & \begin{pmatrix} 0 & -1 & 0 & 0 \\ -1 & 0 & 0 & 0 \\ 0 & 0 & 0 & 0 \\ 0 & 0 & 0 & 0 \end{pmatrix}, \quad S_y = \begin{pmatrix} 0 & 0 & 0 & 0 \\ 0 & 0 & 0 & 0 \\ 0 & 0 & 0 & -1 \\ 0 & 0 & -1 & 0 \end{pmatrix}. \end{aligned} \quad (2)$$

It is convenient to subject the Hamiltonian to a canonical displacement transformation that eliminates terms linear in phonons and generates the inter-center interaction.^{10,11} The

transformed Hamiltonian of the electron subsystem, neglecting dynamic electron-phonon interaction, can be written in the form

$$H_{el} = - \sum_{\substack{m, n, k \\ m \neq n}} \frac{V_{mk} V_{nk}^*}{\hbar \omega_k} \sigma_z^m \sigma_z^n - g_0^2 \bar{\sigma}_z \sum_m \sigma_z^m - \frac{\varepsilon \gamma}{2} \sum_m (1 + \tau_z^m) \sigma_x^m - g \beta \sum_m (H_x S_x^m + H_y S_y^m), \quad (3)$$

where the first two terms describe the inter-center correlations, γ is the factor of the vibronic reduction in the splitting ε and is little different from unity in the case of weak electron-vibration interaction. We note that the Zeeman interaction is not reduced by the vibronic interaction and this important fact will be discussed in more detail below.

In the molecular-field approximation the energy levels are described by the following equation:

$$(A \bar{\sigma}_z - E) \{ \varepsilon^2 (A \sigma_x + E) + (A \bar{\sigma}_z - E) [(A \bar{\sigma}_z + E)^2 - g^2 \beta^2 H_x^2] \} - g^2 \beta^2 H_y^2 [(A \bar{\sigma}_z + E) - g^2 \beta^2 H_x^2] = 0. \quad (4)$$

In Eq. (4), A is the molecular field constant. We first consider the magnetic field oriented along the [110] axis ($H_x \neq 0, H_y = 0$), along which the anomalous field dependence of the magnetic moment is observed experimentally. Since one of the equations contained in (4) is, as previously (as for $H_y \neq 0$) a third-order equation, we shall find the energy levels approximately, on the assumption that $A \bar{\sigma}_z \ll g \beta H_x$ (we consider below in more detail the criterion for this approximation):

$$E_1 = A \bar{\sigma}_z, \quad E_2 = A \bar{\sigma}_z \frac{g^2 \beta^2 H_x^2 - \varepsilon^2 \gamma^2}{g^2 \beta^2 H_x^2 + \varepsilon^2 \gamma^2}, \quad (5)$$

$$E_{3,4} = \pm (\varepsilon^2 \gamma^2 + g^2 \beta^2 H_x^2)^{1/2} - \frac{g^2 \beta^2 H_x^2 A \bar{\sigma}_z}{\varepsilon^2 \gamma^2 + g^2 \beta^2 H_x^2}.$$

By using Eq. (5), it is not difficult to obtain for the \bar{S}_x to which the magnetic moment M_x is proportional ($h_x = g \beta H_x$)

$$S_x = \frac{2h_x}{(h_x^2 + \varepsilon^2 \gamma^2)^{1/2}} \frac{1}{z} \left[\exp \left(\frac{A \bar{\sigma}_z}{kT} \frac{h_x^2 - \varepsilon^2 \gamma^2}{h_x^2 + \varepsilon^2 \gamma^2} \right) \times \left(\operatorname{sh} \frac{(h_x^2 + \varepsilon^2 \gamma^2)^{1/2}}{kT} + \frac{2A \bar{\sigma}_z \varepsilon^2 \gamma^2}{(h_x^2 + \varepsilon^2 \gamma^2)^{3/2}} \operatorname{ch} \frac{(h_x^2 + \varepsilon^2 \gamma^2)^{1/2}}{kT} - \frac{2A \bar{\sigma}_z \varepsilon^2 \gamma^2}{(h_x^2 + \varepsilon^2 \gamma^2)^{3/2}} \exp \left(- \frac{A \bar{\sigma}_z}{kT} \frac{h_x^2 - \varepsilon^2 \gamma^2}{h_x^2 + \varepsilon^2 \gamma^2} \right) \right], \quad (6)$$

$$\bar{\sigma}_z = \frac{1}{z} \left[\frac{2h_x^2}{h_x^2 + \varepsilon^2 \gamma^2} \operatorname{ch} \frac{(h_x^2 + \varepsilon^2 \gamma^2)^{1/2}}{kT} \exp \left(\frac{A \bar{\sigma}_z}{kT} \frac{h_x^2}{h_x^2 + \varepsilon^2 \gamma^2} \right) - \exp \left(- \frac{A \bar{\sigma}_z}{kT} \right) - \frac{h_x^2 - \varepsilon^2 \gamma^2}{h_x^2 + \varepsilon^2 \gamma^2} \exp \left(- \frac{A \bar{\sigma}_z}{kT} \frac{h_x^2 - \varepsilon^2 \gamma^2}{h_x^2 + \varepsilon^2 \gamma^2} \right) \right], \quad (7)$$

$$z = 2 \operatorname{ch} \left[\frac{(h_x^2 + \varepsilon^2 \gamma^2)^{1/2}}{kT} \exp \left(\frac{A \bar{\sigma}_z}{kT} \frac{h_x^2}{h_x^2 + \varepsilon^2 \gamma^2} \right) + \exp \left(- \frac{A \bar{\sigma}_z}{kT} \right) + \exp \left(- \frac{A \bar{\sigma}_z}{kT} \frac{h_x^2 - \varepsilon^2 \gamma^2}{h_x^2 + \varepsilon^2 \gamma^2} \right) \right]. \quad (8)$$

Equation (6) determines the behavior of the magnetic moment M_x || [110] for all magnetic fields and temperatures. The results of a numerical calculation carried out according

to this equation indicate the existence of an inflection in the $\mathcal{M}(H)$ curve at \mathbf{H} || [100]. The calculated field dependence of the effective spin $S_x(H)$ at $T = 4.2$ K and \mathbf{H} || [110] is shown by the points in Fig. 4 (curve 2). The dependence of magnetic moment on S is given by the expression $\mathcal{M}(H) = g \mu S(H)$. The numerical calculations were carried out using the following parameters: $\varepsilon \gamma = 30$ cm, $g = 10$. By varying the parameter A of the inter-center correlation, it was shown that the best agreement with experiment was obtained for $A = 20$ cm⁻¹; we may note that this value of A agrees with that determined⁴ from ultrasonic measurements. The parameters ε and g can be found from the values of the saturation magnetic moment M_0 and the magnetic susceptibility χ at low temperatures and as $H \rightarrow 0$. The values found agree with those determined from independent experiments. It must be pointed out that the actual cell of a TmPO₄ crystal contains two equivalent Tm³⁺ ions, a fact taken into account in the present model by doubling the value of the g -factor. The field variation of the energy levels of Tm³⁺ calculated from Eq. (5) at $T = 10$ K is shown in Fig. 5.

To demonstrate more clearly the role of intercenter Jahn-Teller interaction in bringing about such a magnetic-moment behavior, we look at Eq. (6) at $T = 0$. The value of S_x is then determined by the expression

$$\bar{S}_x = \frac{h_x}{(h_x^2 + \varepsilon^2 \gamma^2)^{1/2}} + \frac{2A \varepsilon^2 \gamma^2 h_x^2}{(h_x^2 + \varepsilon^2 \gamma^2)^3}. \quad (9)$$

It can be seen from Eq. (9) that for $A = 0$ the magnetic moment saturates in the usual way without an inflection. However, for $A \neq 0$ there is an inflection. It is the result of the combination of two types of magnetic nonlinearity. One of them is connected with the noncommutation of the operators of the Zeeman interaction and the crystal field, leading to splitting of the ε -levels of Tm³⁺. The other nonlinearity is produced by correlations of different centers and the mechanism of its action is as follows. The magnetic field H_x which induces a magnetic moment at a crystal site, produces simultaneously a local deformation. However, since the local deformations of Jahn-Teller centers are correlated and influence the magnetic moment, an effective amplification of the magnetic moment arises. From the quantum mechanical point of view the mutual amplification of the magnetic moment and of the deformation is a consequence of commutativity of the operators of the Zeeman interaction and the Jahn-Teller molecular field ($[S_x, \sigma_z] = 0$) and is evidently a general property of systems for which the relations given are satisfied. As a result of this effect the magnetic moment increases faster than linearly with field for not very high magnetic fields, when the correlation nonlinearity mechanism predominates, and the additional term is proportional to H_x^3 as can be seen from Eq. (9). The first nonlinear mechanism is dominant in high magnetic fields and leads to saturation.

As the correlation effects become weaker with increasing temperature, the contribution of the nonlinearity produced by them is reduced, which is in agreement with experiment. It is easy to see this directly from Eqn. (6) by writing it for the case of sufficiently high temperatures, when $A \bar{\sigma}_z \ll kT$, in the form

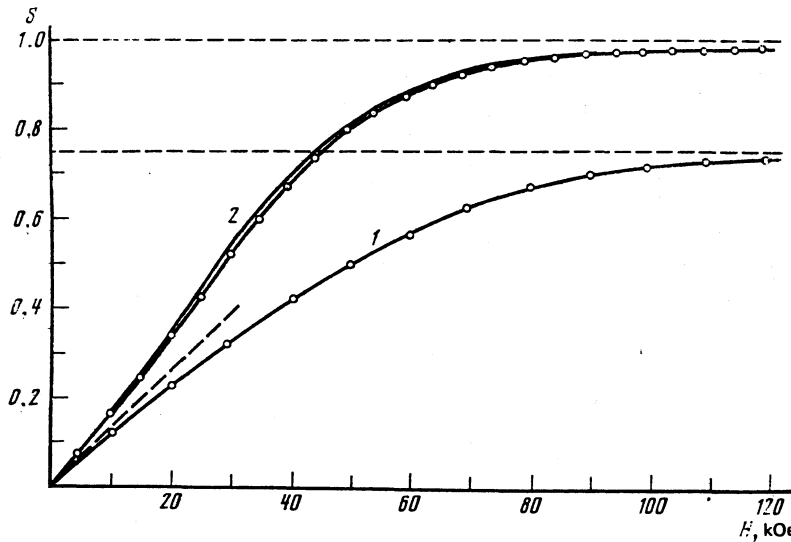


FIG. 4. Calculated variations of effective spin S for TmPO_4 for various orientations of \mathbf{H} : $S_y(H)$ —curve 1 for $\mathbf{H}||[100]$, $S_x(H)$ —curve 2 for $\mathbf{H}||[110]$.

$$S_x = \frac{1}{z} \frac{h_x}{(h_x^2 + \varepsilon^2 \gamma^2)^{1/2}} \left\{ \frac{\text{sh} \frac{(h_x^2 + \varepsilon^2 \gamma^2)^{1/2}}{kT}}{kT} + \frac{2A\bar{\sigma}_z \varepsilon^2 \gamma^2}{(h_x^2 + \varepsilon^2 \gamma^2)^{1/2}} \left[\text{ch} \frac{(h_x^2 + \varepsilon^2 \gamma^2)^{1/2}}{kT} - 1 + \frac{h_x^2}{\varepsilon^2 \gamma^2} \times \frac{(h_x^2 + \varepsilon^2 \gamma^2)^{1/2}}{kT} \text{sh} \frac{(h_x^2 + \varepsilon^2 \gamma^2)^{1/2}}{kT} \right] \right\}, \quad (10)$$

$$\sigma_z = \frac{1}{z} \left\{ \frac{2h_x^2}{h_x^2 + \varepsilon^2 \gamma^2} \left(\text{ch} \frac{(h_x^2 + \varepsilon^2 \gamma^2)^{1/2}}{kT} - 1 \right) + \frac{A\bar{\sigma}_z}{kT} \left[1 + \frac{1}{(h_x^2 + \varepsilon^2 \gamma^2)^2} \left[(h_x^2 - \varepsilon^2 \gamma^2) + 2h_x^4 \text{ch} \frac{(h_x^2 + \varepsilon^2 \gamma^2)^{1/2}}{kT} \right] \right] \right\}, \quad (11)$$

$$Z = 2 \left[1 + \text{ch} \frac{(h_x^2 + \varepsilon^2 \gamma^2)^{1/2}}{kT} + \frac{A\bar{\sigma}_z}{kT} \frac{h_x^2}{h_x^2 + \varepsilon^2 \gamma^2} \times \left(\text{ch} \frac{(h_x^2 + \varepsilon^2 \gamma^2)^{1/2}}{kT} - 1 \right) \right]. \quad (12)$$

As follows from Eq. (10), the contribution of this nonlinear-

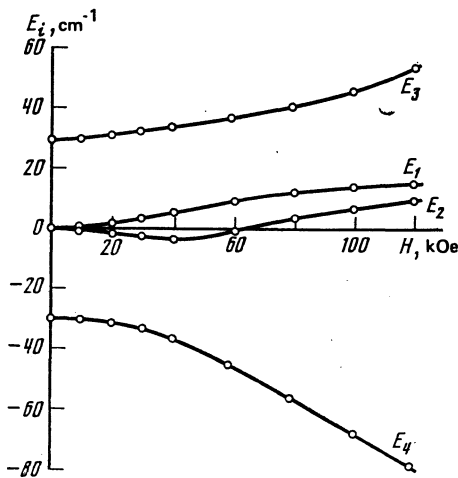


FIG. 5. Magnetic field dependence of electronic energy levels of the Tm^{3+} ion, for $\mathbf{H}||[110]$; $\varepsilon = 30 \text{ cm}^{-1}$, $A = 20 \text{ cm}^{-1}$.

ity is proportional to $\bar{\sigma}_z$, which also causes the corresponding temperature dependence. The field dependences of magnetic moment are shown in Fig. 2 for various temperatures. Comparison of the experimental (Fig. 3) and theoretical dependences of the magnetic susceptibility, described by the expression

$$\chi = \frac{1}{\varepsilon \gamma} \text{sh} \frac{\varepsilon \gamma}{kT} \left(\text{ch} \frac{\varepsilon \gamma}{kT} + 1 \right)^{-1},$$

showed good agreement.

We shall discuss the accuracy of the approximation $A\bar{\sigma}_z \ll h_x, \varepsilon \gamma$ used in finding the energy levels of the Tm^{3+} ion. It is evidently most difficult to have this inequality satisfied at $T = 0$. In this case the corresponding criterion of the form

$$Ah_x^2 / (h_x^2 + \varepsilon^2 \gamma^2) \ll h_x, \varepsilon \gamma. \quad (13)$$

In the weak field region, where $h_x \ll \varepsilon \gamma$, the inequality (13) is clearly satisfied, since

$$Ah_x \ll \varepsilon^2. \quad (14)$$

In the strong field region, where $h_x \gg \varepsilon \gamma$, the inequality (13) can be expressed in the form

$$A \ll h_x, \quad (15)$$

$$A \ll \varepsilon \gamma. \quad (16)$$

The first of these inequalities is easily satisfied. However, the parameters A and $\varepsilon \gamma$ can satisfy (and this is realized in TmPO_4) a weaker inequality $A < \varepsilon \gamma$, which is in fact the condition for the impossibility of achieving a structural phase transition. Finally, in the region of intermediate fields, the criterion (13) takes the form

$$A \ll 2\varepsilon \gamma, \quad (17)$$

while only the condition

$$A < \varepsilon \gamma \quad (18)$$

is reliably realized. For high ($h_x \gg \varepsilon \gamma$) and intermediate ($h_x \sim \varepsilon \gamma$) fields the criterion of Eq. (13) is thus not very well

satisfied. However, it should be borne in mind that the maximum fields ($H_x \sim 120$ kOe) used in the experiments correspond to only the intermediate region $H_x \sim \varepsilon\gamma$. In this region, taking the obtained value $A = 20 \text{ cm}^{-1}$, we have $A/2\varepsilon\gamma = 1/3$. Finally, it must be realized that the experiments were carried out at finite temperatures for which the conditions for the validity of the approximation used are not as stringent as (13). The accuracy of the approximation can be ultimately estimated after a numerical solution of the cubic equation in (4), and from the analysis it can be assumed that the error produced by using the approximation is not above 15 to 20%.

It follows from everything said above that the existence of an inflection in the field dependence of $\mathcal{M}(H)$ is a characteristic of crystals of the TmPO_4 type, for which the parameter A is comparable with $\varepsilon\gamma$, $A \lesssim \varepsilon\gamma$. The local Jahn-Teller distortion correlation parameter, which is very important for these systems, can be found by determining the magnitude of the field corresponding to the inflection, from magnetic measurements. An analytic dependence of A on the magnetic field h_x^i at the inflection of the $\mathcal{M}(H)$ curve can be obtained for $T = 0$:

$$A = \frac{1}{4} \frac{(h_x^i)^2 + \varepsilon^2 \gamma^2}{\varepsilon^4 \gamma^4 + 2h_x^i \varepsilon^2 \gamma^2 - 5\varepsilon^2 \gamma^2 h_x^i n^2}. \quad (19)$$

It is not difficult to verify that we can find $A \approx 20 \text{ cm}^{-1}$ for TmPO_4 by using the h_x^i . The dependence⁷ of γ on H gives, in general, a contribution to the field dependence of magnetic moment, but the good agreement with experiment of the model in which this is not taken into account indicates that this effect is small. We shall now consider the behavior of the magnetic moment of a TmPO_4 crystal when the magnetic field is oriented along the [100] axis. For this $H_x = H_y = H_0/\sqrt{2}$ must be substituted into the original Hamiltonian (Eq. (1)). Equation (4), which describes the energy levels of the Tm^{3+} ion in the molecular field approximation, takes the form ($h_0 = g\beta H_0$)

$$(A^2 \bar{\sigma}_z^2 - E^2)^2 + \varepsilon^2 \gamma^2 (A^2 \bar{\sigma}_z^2 - E^2) - H_0^2 (A^2 \bar{\sigma}_z^2 + E^2) + \frac{1}{4} h_0^4 = 0. \quad (20)$$

The solution of this biquadratic equation is described by the expressions

$$E_{1,3} = \pm \left\{ A^2 \bar{\sigma}_z^2 - \frac{h_0^2}{2} + \frac{\varepsilon^2 \gamma^2}{2} + \left[\frac{\varepsilon^4 \gamma^4}{4} + \frac{h_0^2}{2} (4A^2 \bar{\sigma}_z^2 + \varepsilon^2 \gamma^2) \right]^{1/2} \right\}^{1/2}, \quad (21)$$

$$E_{2,4} = \pm \left\{ A^2 \bar{\sigma}_z^2 - \frac{h_0^2}{2} + \frac{\varepsilon^2 \gamma^2}{2} + \left[\frac{\varepsilon^4 \gamma^4}{4} + \frac{h_0^2}{2} (4A^2 \bar{\sigma}_z^2 + \varepsilon^2 \gamma^2) \right]^{1/2} \right\}^{1/2}.$$

The value of $\bar{\sigma}_z$ can be found by using Eq. (21). Analysis of the corresponding expression shows that in the absence of a structural phase transition in a zero magnetic field, as a result of the relation between the parameters $A < \varepsilon\gamma$, deformation of a crystal of B_{2g} symmetry does not arise (moreover, a field having the orientation considered only reduces the deformation, if it exists). We must therefore put $\bar{\sigma}_z = 0$ in Eq. (21). Allowing for this, we obtain for the value of \bar{S}_{xy} , which determines the magnetic moment for $\mathbf{H} \parallel [100]$,

$$S_{xy} = \frac{h_0}{2} \left(\frac{1+B^{-1}}{E_1} \text{sh} \frac{E_1}{kT} + \frac{1-B^{-1}}{E_2} \text{sh} \frac{E_2}{kT} \right), \quad (22)$$

$$E_{1,2} = \left(\frac{1}{2} h_0^2 + \frac{\varepsilon^2 \gamma^2}{2} (1 \pm B) \right)^{1/2}, \quad B = (1 + 2h_0^2/\varepsilon^2 \gamma^2)^{1/2}, \quad (23)$$

$$Z = 2 \left(\text{ch} \frac{E_1}{kT} + \text{ch} \frac{E_2}{kT} \right). \quad (24)$$

The $\bar{S}_{xy}(H_0)$ dependences are shown graphically in Fig. 4. In agreement with experiment, there is no inflection on these curves and the usual saturation occurs in high magnetic fields. This result is fully understandable within the framework of the considerations given above, since a magnetic field in this orientation, as pointed out, does not produce a B_{2g} -symmetry deformation, so that the nonlinear correlation mechanism is switched off. This is easy to see by using the expression for S_{xy} at $T = 0$, which takes the form

$$\bar{S}_{xy} = h_0 \left[1 + \left(1 + \frac{2h_0^2}{\varepsilon^2 \gamma^2} \right)^{-1/2} \right] \times 2 \left\{ \frac{h_0^2}{2} + \frac{\varepsilon^2 \gamma^2}{2} \left[1 + \left(1 + \frac{2h_0^2}{\varepsilon^2 \gamma^2} \right)^{1/2} \right] \right\}^{-1/2}. \quad (25)$$

It follows that in the region of small fields, where $h \ll \varepsilon\gamma$,

$$\bar{S}_{xy} = \frac{h_0}{2} \left(1 - \frac{3}{2} \frac{h_0^2}{\varepsilon^2 \gamma^2} \right), \quad (26)$$

which corresponds to the usual $\mathcal{M}(H)$ behavior for saturation. One more result which clarifies the experiments can easily be obtained from Eq. (25). From the measurements it follows that the value of the saturation magnetic moment for $\mathbf{H} \parallel [100]$ is appreciably smaller than the corresponding moment for $\mathbf{H} \parallel [110]$. In fact, it follows from Eq. (25) that $\bar{S}_{xy} \rightarrow 1/\sqrt{2}$ as for $h_0 \rightarrow \infty$, while $\bar{S}_x \rightarrow 1$.

The ratio $\bar{S}_x/\bar{S}_{xy} = \sqrt{2}$ is in good agreement with experiment.

The analysis shows that the anomalies found in the magnetic properties of TmPO_4 are satisfactorily explained by taking account of the correlation of local Jahn-Teller distortions. There are grounds for supposing that the features of the behavior of HoVO_4 in a magnetic field (Fig. 1) are also produced by this effect. However, the difference between the electronic spectra of Ho^{3+} in HoVO_4 and of Tm^{3+} in TmPO_4 make direct application of the results given above impossible, so that this case requires separate consideration.

In the present work an anomalous field dependence of the magnetic moment of TmPO_4 has thus been found, characterized by the existence of an inflection in the $\mathcal{M}(H)$ curve. A model has been constructed, based on a cooperative Jahn-Teller effect, which connects the existence of this anomaly with the correlation of local Jahn-Teller distortions at different centers. The crystal splitting $\varepsilon\gamma$, the g -factor, and the correlation parameter A have been determined as a result of the investigations carried out.

The authors thank P. L. Kapitza and A. S. Borovik-Romanov for their interest and D. I. Khomskii and B. Z. Malkin for discussion of the results.

¹International laboratory for high magnetic fields and low temperatures, Wroclaw, Poland.

²The authors thank I. A. Bondar' and L. P. Mezentseva for kindly supplying the crystals.

³The authors thank Yu. F. Orekhov for determining the single-crystal orientations.

¹G. A. Gehring and K. A. Gehring, *Rep. Prog. Phys.* **38**, 1 (1975).

²R. J. Elliott, R. T. Harley, W. Hayes, and S. R. P. Smith, *Proc. R. Soc. London Ser. A* **328**, 217 (1972).

³R. T. Harley, C. H. Perry, and W. J. Richter, *J. Phys. C* **10**, L187 (1977).

⁴R. T. Harley and D. I. Manning, *J. Phys. C* **11**, L633 (1978).

⁵F. Mehran, T. S. Plaskett, and K. W. H. Stevens, *Phys. Rev. B* **16**, 1 (1977).

⁶J. E. Battison, M. J. M. Leask, J. B. Lowry, and A. Kasten, *J. Phys. C* **9**, 2295 (1976).

⁷V. A. Ioffe, S. I. Andronenko, I. A. Bondar', L. P. Mezentseva, A. N. Bazhan, and C. Bazan, *Pis'ma Zh. Eksp. Teor. Fiz.* **34**, 586 (1981) [*JETP Lett.* **34**, 562 (1981)].

⁸A. Abragam and B. Bleaney, *Electron Paramagnetic Resonance of Transition Ions*, Clarendon Press, Oxford (1970).

⁹A. N. Bazhan, A. S. Borovik-Romanov, and N. M. Kreines, *Prib. Tekh. Eksp. No. 1*, 213 (1973) [*Instrum. and Exp. Tech.* **16**, 261 (1973)].

¹⁰R. J. Elliott, *Proc. Intern. Conf. on Light Scattering in Solids, Paris 1971*, Ed. M. Balkanski, Flammarion et Cie, Paris, p. 354.

¹¹B. G. Vechter and M. D. Kaplan, *Phys. Lett.* **43A**, 389 (1973).

Translated by R. Berman